Estimation of Electron-Phonon Coupling Parameters from Low-temperature Optical Spectra

Mike Reppert
I-Center report for independent study under Dr. Virginia Naibo (KSU Department of Mathematics) and Dr. Ryszard Jankowiak (KSU Department of Chemistry)

I. Introduction and statement of the problem

In low-temperature spectroscopy, one is often interested in learning how strongly a chromophore interacts with its host matrix[*]. For example, by studying dye molecules embedded in frozen solutions or glassy matrices, one can learn interesting information about the matrix itself. Of more immediate interest for us is that the interaction of chromophores with their environment can have important consequences on the electronic properties of the chromophore itself, altering its optical (absorption and emission) spectra as well as coupling and energy transfer rates between chromophores. The particular system in which we are interested is the Photosystem II (PSII) chlorophyll-protein complex, consisting of a set of chlorophyll molecules (the chromophores) embedded in a protein "matrix." Since we are interested in understanding how PSII functions in harvesting solar energy for photosynthesis, it is important to understand how the chlorophyll molecules interact both with each other (inter-molecular coupling and energy transfer) and with their environment. Knowledge of such properties can, for example, be used to model the optical and electronic properties of photosynthetic complexes[1-3], giving detailed insight on its function in photosynthesis.

Essentially, what we are interested in here is how transitions between the eigenstates of a chromophore affect (and are affected by) the vibrational motions of the matrix. A molecule can undergo several types of eigenstate transitions: usually we are interested in *vibrational transitions* and *electronic transitions* (which involve changes in the distribution of electrons within the molecule and are much more energetic than vibrational transitions). When a molecule undergoes a transition from one eigenstate to another, its interaction with the environment can trigger changes in the vibrational eigenstates of the environment—which we call *phonons*—as well. Since matrix phonons and molecular vibrational transitions are of roughly similar energies, they can each induce changes in each other—a phonon interacting with the molecule can trigger vibrational transitions, and a molecular vibrational transition can cause the creation or annihilation of a matrix phonon. Because electronic transitions are much more energetic than vibrational transitions, matrix phonons are very unlikely to induce molecular electronic transitions, but a molecular electronic transition can easily create or destroy matrix phonons. This interaction is termed *electron-phonon coupling*, and is an important feature of low-temperature spectroscopy. Several important parameters describing electron-phonon coupling (which can be obtained by low-temperature

[*] In this context, a "chromophore" is any kind of molecule that absorbs light, and a "matrix" is whatever kind of material the chromophore happens to be embedded in. For example, if we were studying a frozen solution of Kool-Aid, the "chromophore" is the Kool-Aid molecules, and the matrix is the water in which those molecules are frozen.

spectroscopy) are the *Franck-Condon*, *Debye-Waller*, and *Huang-Rhys* factors (usually denoted FC, α, and S, respectively; all are dimensionless constants). A detailed description of these processes can be found in Ref [4]; only a brief description is needed here.

Figure 1 shows a typical absorption spectrum of a single molecule embedded in a host matrix. The vertical axis represents the probability that the wavefunction of the system will undergo a transition from the lowest-energy eigenstate (ground state) to a higher-energy eigenstate when exposed to photons of light with the energy corresponding to the frequency given on the horizontal axis. As can be seen in Figure 1, this *single-site spectrum* has two major features: a sharp and very narrow *zero phonon line* (ZPL) and a much broader *phonon sideband* (PSB), which occurs at higher frequencies from the ZPL. (In fact, there are likely to be other peaks occurring at higher frequencies corresponding to intramolecular vibrational transitions coupled to this electronic transition, but we will not consider these here).

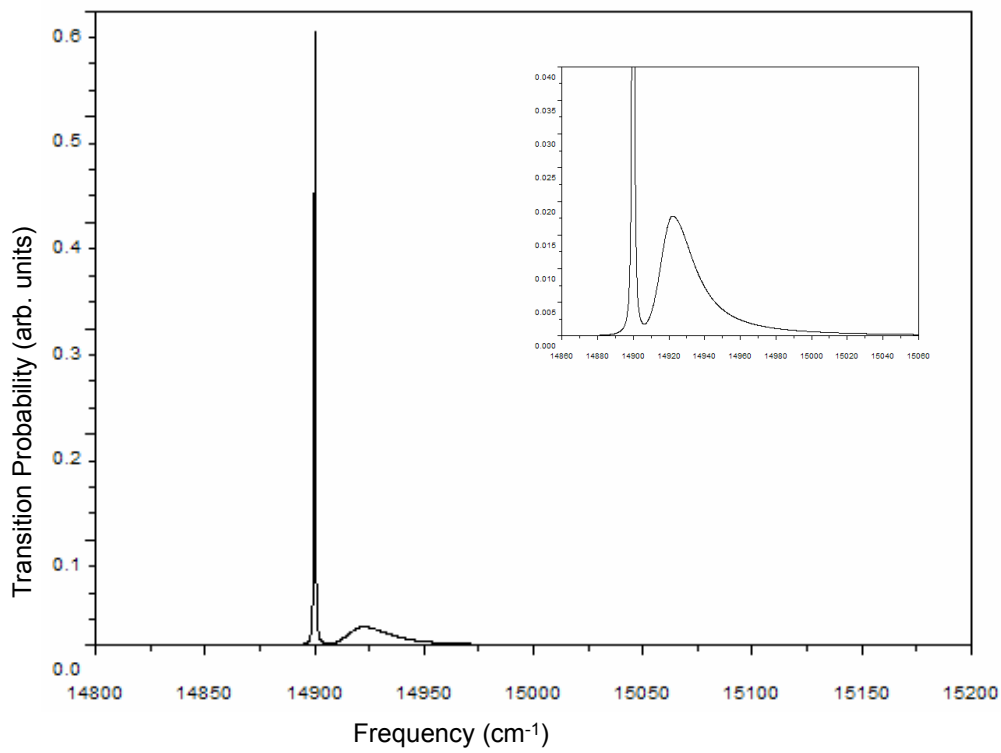

Figure 1. Calculated single-site spectrum for a hypothetical pigment having a pure electronic transition (zero-phonon line) at 14900 cm^{-1}.

Physically, the ZPL corresponds to transitions which do *not* induce any changes in the vibrational modes (phonons) of the matrix, i.e. *the electronic transition occurs with no interaction with the matrix phonons*, while the PSB corresponds to *electronic transitions which occur via interaction with matrix phonons*. From time-dependent perturbation theory[5], it can be shown theoretically that this peak will have the shape of a Lorentzian function (Lorentz-Cauchy distribution) with the general formula

$l(\Omega-\omega)=\frac{1}{\pi}\cdot\frac{\Gamma}{(\omega-\Omega)^2+\Gamma^2}$. The parameter Γ is the full width of the Lorentzian measured at half-maximum, and depends on the lifetime of the excited state of the molecule (i.e. how long it takes for the transition to occur). Experimentally, the shape of the ZPL is relatively easy to determine via hole-burning (HB) or fluorescence line narrowing (FLNS) spectroscopy, among other methods since (up to scaling by a constant) it depends only on this one parameter. The PSB, unfortunately, is more complicated to describe theoretically, and is somewhat more difficult to obtain experimentally since there is no single formula which can be used to fit the data.

The relative intensities of these two features in the single-site spectrum represent the electron-phonon coupling strength (how strongly molecular electronic transitions interact with matrix phonons). Physically, the ZPL represents all transitions which occur without interaction with matrix phonons; the PSB represents all those electronic transitions which can occur only through creation or annihilation of matrix phonons. Hence, if the integral of the ZPL is very large with respect to the integral of the PSB, this indicates that most electronic transitions occur without interacting with matrix phonons: in this case, we say that electron-phonon coupling is weak. On the other hand, if the integral of the ZPL is small with respect to the integral of the PSB, this indicates that most electronic transitions occur via interaction with matrix phonons, and we say that electron-phonon coupling is strong. In the limit as temperature approaches 0 Kelvins, we have the following relations:

$$\alpha = e^{-S} = \frac{I_{ZPL}}{I_{ZPL}+I_{PSB}},$$

where α is the Debye-Waller factor, S is the Huang-Rhys factor, and I_{ZPL} and I_{PSB} are the integrated areas under the ZPL and PSB, respectively. In the weak-coupling limit, $I_{PSB} \to 0$, $\alpha \to 1$, and $S \to 0$. Conversely, in the strong-coupling limit, $\alpha \to 0$, and $S \to \infty$. In general, when $S < 1$ we say that electron-phonon coupling is "weak," and when $S > 1$, we say that electron-phonon coupling is "strong."

The spectrum shown in Figure 1 represents the absorption of a single molecule. However, actually making measurements on single molecules is experimentally very difficult; it is much easier to make "bulk" measurements, in which one measures at the same time the absorption of many molecules in a sample. Unfortunately, bulk measurements complicate the picture a bit. Unless we are working with molecules embedded in a perfect crystal lattice, the immediate environment of each molecule is likely to be slightly different. As a result, although roughly similar, the precise energies of the eigenstates of each molecule are likely to be slightly different, causing their single-site absorption spectra to be shifted slightly relative to each other. Figure 2A shows a hypothetical absorption spectrum which might be obtained by measuring simultaneously the absorption of 5 chromophores with slightly different peak absorption frequencies (ZPL frequencies) ranging from 14800 to 15200 cm^{-1}. The bulk samples that are experimentally convenient to work with, on the other hand, consist of millions of individual molecules, each with its own single-site absorption spectrum. Because each molecule is of the same type, the variations in their ZPL peak frequencies are random, so

that the ZPL peak frequencies generally fall in a Gaussian (normal) distribution around some center frequency. The result is an *inhomogenously broadened* absorption spectrum, such as the ones shown in Frames B and C of Figure 2. Frame B shows a hypothetical spectrum calculated for a solution containing only 50 individual molecules, while Frame C (black curve) shows the theoretical limit as the number of molecules approaches infinity.

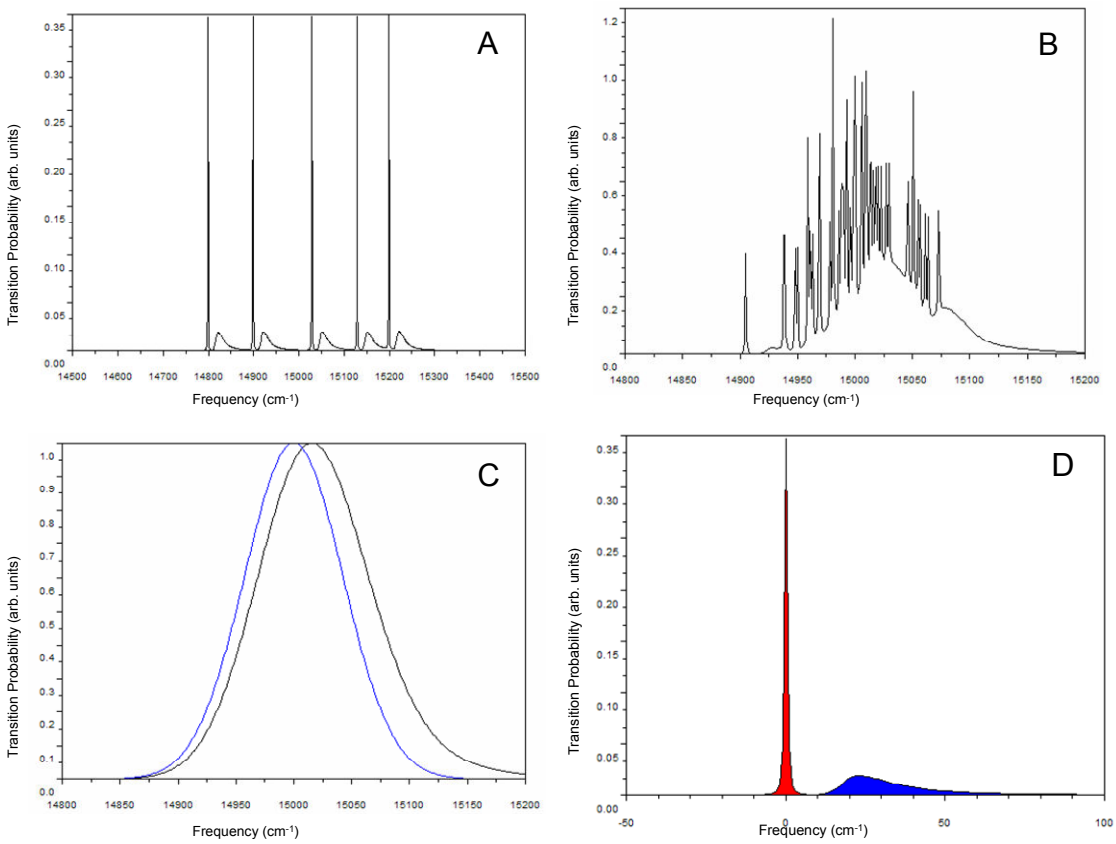

Figure 2. **Frame A**: calculated spectrum for the electronic transitions of five (non-interacting) molecules with transition energies (ZPL peak frequencies) scattered around 15000 cm^{-1}. **Frame B**: calculated absorption spectrum for a sample of 50 molecules with electronic transitions placed in a Gaussian distribution around 15000 cm^{-1}. **Frame C**: (black curve) calculated absorption spectrum for a sample with an infinite number of molecules with electronic transitions placed randomly within the Gaussian probability distribution function (blue curve); the black curve is simply the convolution of a single-site absorption spectrum (Frame D) with the distribution function (blue curve). **Frame D**: single-site absorption spectrum used in calculations in Frames A – C. The red shaded area is the integral of the ZPL; the blue shaded area is the integral of the PSB.

The blue curve in Frame C is a Gaussian Site Distribution Function (SDF): the definite integral from v_1 to v_2 gives the probability that a given chromophore will have a peak absorption frequency somewhere between v_1 and v_2. The black curve is the

convolution of this function with a single-site absorption spectrum which has a ZPL peak at 0 cm^{-1}, as shown in Frame D of Figure 2. An inhomogenously broadened spectrum such as the black curve in Frame C is referred to as a "bulk" spectrum since it is the result of measurements made on "bulk" samples, rather than on individual molecules.

As mentioned earlier, it is extremely difficult experimentally to directly measure the true single-site spectrum for most chromophores. On the other hand, measurement of bulk spectra (i.e. spectra obtained for "bulk" samples, consisting of many thousands of distinct molecules), such as the bulk absorption spectrum shown in Figure 2C is relatively easy. By means of hole-burning (HB) spectroscopy, one can also, in many cases, obtain an accurate SDF for a system. Since the bulk spectrum is just the convolution of the SDF with the single-site spectrum, this begs the question of whether one can use a deconvolution procedure to extract an accurate single-site absorption spectrum from only the bulk spectrum and the SDF. On the other hand, for some systems, it is possible to measure the single-site spectrum more easily than to obtain an accurate SDF. In these cases, it might be useful to be able to extract the SDF from the bulk spectrum and single-site spectrum. These are the two questions which we wish to address.

Mathematically, we can state the problem as follows. We have three functions: a site distribution function $G(\omega-\Omega_0)$ (a Gaussian centered at Ω_0), a single-site spectrum $F(\omega)$ (the sum of the ZPL and PSB functions), and a bulk spectrum $E(\omega)$ (an experimentally measured absorption or emission spectrum). For consistency in what follows, it will be convenient to scale each of these functions such that each has an integral intensity of unity. That is,

$$\int_{-\infty}^{\infty} G(\omega-\Omega_0)d\omega = \int_{-\infty}^{\infty} F(\omega)d\omega = \int_{-\infty}^{\infty} E(\omega)d\omega = 1.$$

As mentioned earlier, $E(\omega)$ is just the convolution of $G(\omega-\Omega_0)$ with $F(\omega)$:

$$E = G * F.$$

Furthermore, $F(\omega)$ is just the sum of the ZPL and PSB functions, $L(\omega)$ and $P(\omega)$, that is,

$$F(\omega) = L(\omega) + P(\omega).$$

Here $L(\omega)$ is a Lorentzian centered at 0 with integral I_{ZPL}, (i.e. $L(\omega) = \frac{I_{ZPL}}{\pi} \cdot \frac{\Gamma}{\omega^2+\Gamma^2}$), and $P(\omega)$ is an experimentally obtained side band function with integral I_{PSB}. For convenience, we define two functions $l(\omega)$ and $p(\omega)$ which both have integrals of unity, so that $L(\omega) = I_{ZPL}\, l(\omega)$ and $P(\omega) = I_{ZPL}\, p(\omega)$, giving

$$F(\omega) = I_{ZPL}\, l(\omega) + I_{ZPL}\, p(\omega)$$

Recalling that $\int_{-\infty}^{\infty} F(\omega)d\omega = 1$ and that $\alpha = e^{-S} = \frac{I_{ZPL}}{I_{ZPL}+I_{PSB}}$, we obtain

$$\alpha = e^{-S} = \frac{I_{ZPL}}{I_{ZPL} + I_{PSB}} = I_{ZPL}\,.$$

II. Possible methods

<u>Method 1: Deconvolution to obtain F</u>

Where we proceed from here depends on what experimental information we have available. In the simplest case, suppose that we have accurate experimental curves for *G* and for *E*, but have no information on *F*. Taking the Fourier transform (FT) of both sides of our simple equation, $E = G * F$, we obtain

$$\hat{E} = \hat{G} \cdot \hat{F}$$

where we have used the property that the FT of the convolution of two functions is just the product of the FTs of the two functions. Assuming certain constraints on *E* and *G*, we can divide both sides by $\hat{G}$ to obtain

$$\hat{F} = \frac{\hat{E}}{\hat{G}} \rightarrow F = IFT\left(\frac{\hat{E}}{\hat{G}}\right),$$

where "IFT( )" represents the inverse Fourier transform.

Unfortunately, since experimentally measured curves invariably contain some noise, it is unlikely that a procedure of this kind can directly return an accurate single-site absorption spectrum. For example, a preliminary attempt using real data from the Jankowiak lab is shown in Figure 3. Frame A shows the measured emission spectrum (*E*; black curve) and the SDF (*G*; blue curve) of the lowest energy chlorophyll state of the CP47 core antenna complex of Photosystem II (a chlorophyll-containing protein involved in oxygenic photosynthesis). Frame B shows the spectrum obtained when *E* and *G* are directly deconvolved using numerical FT as above (the scale is arbitrary; probably the large spike near 262 should correspond to 0 cm^{-1}). Calculations were performed in Scilab 4.1.1 using the `fft()` and `ifft()` commands.

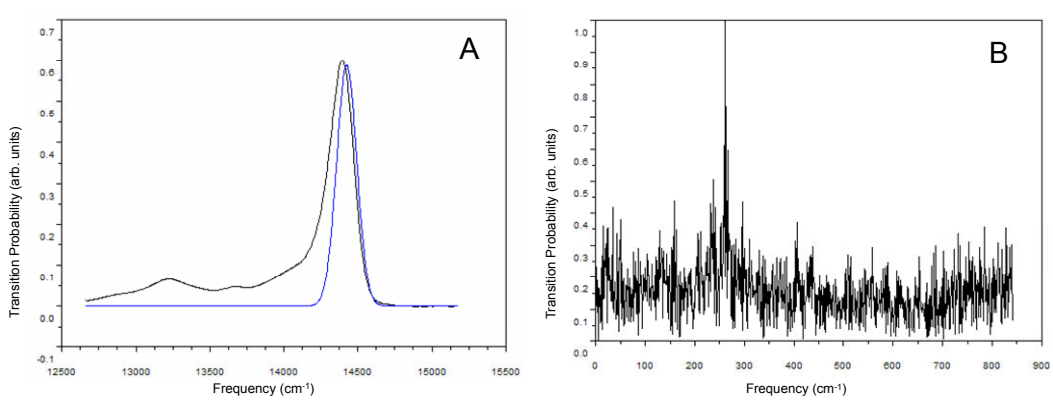

Figure 3. **Frame A**: experimental bulk emission spectrum (black curve) and Gaussian approximation of the SDF (blue curve) for the lowest-energy state of the CP47 antenna complex of photosystem II. **Frame B**: "single-site" absorption spectrum obtained by numerical deconvolution of the two curves in Frame A.

As seen in Frame B, there is far too much noise in the obtained single-site" spectrum for the method to be useful in this way. The major problems here are probably (1) experimental noise in the measured emission spectrum (although it cannot be seen in Figure 3, close examination of individual points reveals significant noise) and (2) an inaccurate SDF. The SDF presents a particular problem for the CP47 complex because, for physical reasons, the SDF is probably not a true Gaussian, and the exact shape cannot be easily measured experimentally. Nonetheless, the method could possibly be useful for simpler systems in which the emission spectrum can be obtained with less noise and for which the SDF is a true Gaussian (or can at least be measured more precisely). At present, we are looking for such a simple system (in the lab) with which to test the method.

Method 2: Deconvolution to obtain the distribution function

On the other hand, suppose that we can measure the single-site absorption spectrum and the emission spectrum; it is a simple matter to use a deconvolution to obtain the SDF, as shown in Figure 4. The blue curve is the experimentally measured emission spectrum, while the black curve is the estimated SDF obtained by deconvolution of the emission spectrum from a calculated single site absorption (such as the one shown in Figure 2D) based on experimentally estimated values for the Huang-Rhys factor S and phonon sideband shape. (The additional broad peaks to lower frequency from the main peak are due to vibronic transitions). Such a procedure is quite easy, and in certain circumstances could be useful, although since it is usually experimentally more difficult to obtain the single-site spectrum than the SDF, its scope is limited.

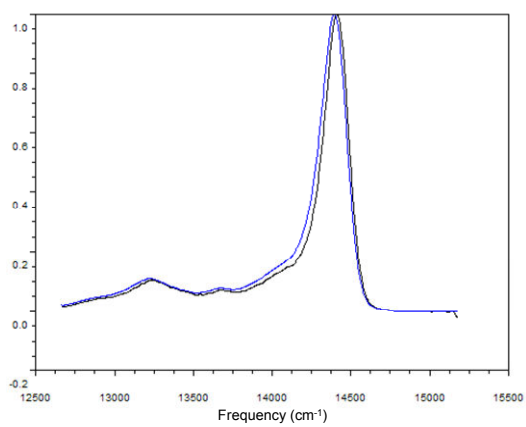

Figure 4. Measured bulk emission spectrum (blue curve; see Figure 3 A) and calculated SDF (black curve) obtained by numerical deconvolution of the emission spectrum with the calculated single-site absorption spectrum shown in Figure 2 D.

Method 3: Estimating *S* using an experimentally determined PSB shape, SDF, and bulk spectrum

One final possibility is that we might be able to experimentally obtain the shape of the PSB and ZPL (that is, curves $p(\omega)$ and $l(\omega)$ from above), but not the constants I_{ZPL}

and I_{PSB}. Assuming that we can measure the SDF and a bulk absorption/emission spectrum, we can rearrange as follows to obtain the Huang-Rhys factor S:

$$
\begin{aligned}
& E = G * F = I_{ZPL} G * l(\omega) + I_{PSB} G * p(\omega) \\
& \rightarrow \hat{E} = I_{ZPL} \hat{G} \cdot \hat{l}(\omega) + I_{PSB} \hat{G} \cdot \hat{p}(\omega) \\
& \rightarrow \hat{E} = \hat{G} \cdot \left(I_{ZPL} \hat{l}(\omega) + I_{PSB} \hat{p}(\omega) \right) \\
& \rightarrow \frac{\hat{E}}{\hat{G}} = I_{ZPL} \hat{l}(\omega) + I_{PSB} \hat{p}(\omega)
\end{aligned}
$$

Recalling that $I_{ZPL} + I_{PSB} = 1 \rightarrow I_{PSB} = 1 - I_{ZPL}$, we obtain

$$
\begin{aligned}
& \frac{\hat{E}}{\hat{G}} = I_{ZPL} \hat{l}(\omega) - I_{ZPL} \hat{p}(\omega) + \hat{p}(\omega) \\
& \rightarrow \frac{\hat{E}}{\hat{G}} = I_{ZPL} \left(\hat{l}(\omega) - \hat{p}(\omega) \right) + \hat{p}(\omega)
\end{aligned}
$$

Choosing some frequency ω for which $\hat{l}(\omega) \neq \hat{p}(\omega)$, we have

$$
\frac{\frac{\hat{E}}{\hat{G}} - \hat{p}(\omega)}{\left(\hat{l}(\omega) - \hat{p}(\omega) \right)} = I_{ZPL} = \alpha = e^{-S} .
$$

Of course, since this method relies on the same function $\frac{\hat{E}}{\hat{G}}$ as does Method 1, it is subject to the same problems with experimental noise and measurement errors. In addition, since it requires knowledge of the PSB function $\hat{p}(\omega)$ and since Method 1 provides, in the end, the same information (after integrating the PSB and ZPL obtained from the single-site spectrum), it remains to be seen whether this method will be of any practical use, aside from providing a direct and convenient way to calculate S. It is hoped, however, that in situations where $\hat{p}(\omega)$ is experimentally available, this method (or one like it) can be used to obtain a more accurate estimate of S than would be obtained by the rather crude data manipulation in Method 1.

III. Conclusion

As described above, each of these three methods are strongly dependent on the quality of experimental data. Although Methods 1 and 3 can, in principle, provide very detailed information on the system from very easily obtained experimental information, experimental noise and uncertainty are likely to make these methods unusable for most systems. At present, we are investigating the applicability of this method to several simple systems for which we can obtain very reliable experimental data.

Method 2, on the other hand, is less subject to problems with experimental noise since the single-site spectrum used will likely be modeled with an analytical function, giving zero noise for $F(\omega)$. On the other hand, however, the information obtained (the

SDF for the system) can in most circumstances be obtained through simpler experimental means. One possible application for this method would be for systems in which the SDF is not a Gaussian function; for example, in certain photosynthetic complexes (CP43 and CP47 of Photosystem II are two examples[1, 6, 7]) the presence of energy transfer between individual pigments causes the SDF of the lowest energy state of the complex to be non-Gaussian. Whereas Gaussian SDFs are relatively easy to obtain experimentally since only two parameters (standard deviation and peak position) are needed to fully specify the entire curve, these non-Gaussian SDFs are more unpredictable. In these cases, Method 2 could well prove useful; we are currently investigating whether it can be used to obtain the true SDF for the lowest-energy state of the CP47 antenna complex of Photosystem II.

For all three methods, further work is required before they become convenient to use for many systems. It is hoped, however, that with some refinement and revision, these methods (or others like them) could provide a useful process for converting experimental data into easily usable information.

References

(1) Reppert, M.; Zazubovich, V.; Dang, N. C.; Seibert, M.; Jankowiak, R. Low-Energy Chlorophyll States in the CP43 Antenna Protein Complex: Simulation of various Optical Spectra. II. *J Phys Chem B* **2008**, *112*, 9934-9947.

(2) Novoderezhkin, V. I.; Dekker, J. P.; van Grondelle, R. Mixing of Exciton and Charge-Transfer States in Photosystem II Reaction Centers: Modeling of Stark Spectra with Modified Redfield Theory. *Biophys. J.* **2007**, *93*, 1293-1311.

(3) Raszewski, G.; Renger, T. Light Harvesting in Photosystem II Core Complexes is Limited by the Transfer to the Trap: Can the Core Complex Turn into a Photoprotective Mode? *J. Am. Chem. Soc.* **2008**, *130*, 4431-4446.

(4) Jankowiak, R. Fundamental Aspects of Fluorescence Line-Narrowing Spectroscopy. *Chemical Analysis (New York)* **2000**, *156*, 235-271.

(5) Sakurai, J. J. In Tuan, S. F., Ed.; Modern Quantum Mechanics, Revised Edition; Addison-Wesley Publishing Company: 1994; pp 325-345.

(6) Zazubovich, V.; Jankowiak, R. On the Energy Transfer between Quasi-Degenerate States with Uncorrelated Site Distribution Functions: An Application to the CP43 Complex of Photosystem II. *Journal of Luminescence,* **2007**, *127*, 245-250.

(7) Dang, N. C.; Zazubovich, V.; Reppert, M.; Neupane, B.; Picorel, R.; Seibert, M.; Jankowiak, R. The CP43 Proximal Antenna Complex of Higher Plant Photosystem II Revisited: Modeling and Hole Burning Study. I. *J Phys Chem B* **2008**, *112*, 9921-9933.